Supporting Information

Unveiling the Critical Role of Ammonium Bromide in Blue Emissive Perovskite Films

Xuechun Wang[a], Lei Cai[a], Yatao Zou*[a], Dong Liang[a, b], Lu Wang[a], Ya Li[a], Jiaqing Zang[a], Guilin Bai[a], Xingyu Gao[b], Tao Song*[a], Baoquan Sun*[a, c]

[a.] Jiangsu Key Laboratory for Carbon-Based Functional Materials & Devices, Institute of Functional Nano & Soft Materials (FUNSOM), Joint International Research Laboratory of Carbon-Based Functional Materials and Devices, Soochow University, 199 Ren'ai Road, Suzhou, 215123, Jiangsu, China.
E-mail: yataozousuda@163.com; tsong@suda.edu.cn; bqsun@suda.edu.cn

[b.] Shanghai Synchrotron Radiation Facility (SSRF), Shanghai Institute of Applied Physics, Chinese Academy of Sciences, 239 Zhangheng Road, Pudong New Area, Shanghai 201204, China.

[c.] Macao Institute of Materials Science and Engineering, Macau University of Science and Technology, Taipa 999078, Macau SAR, China.

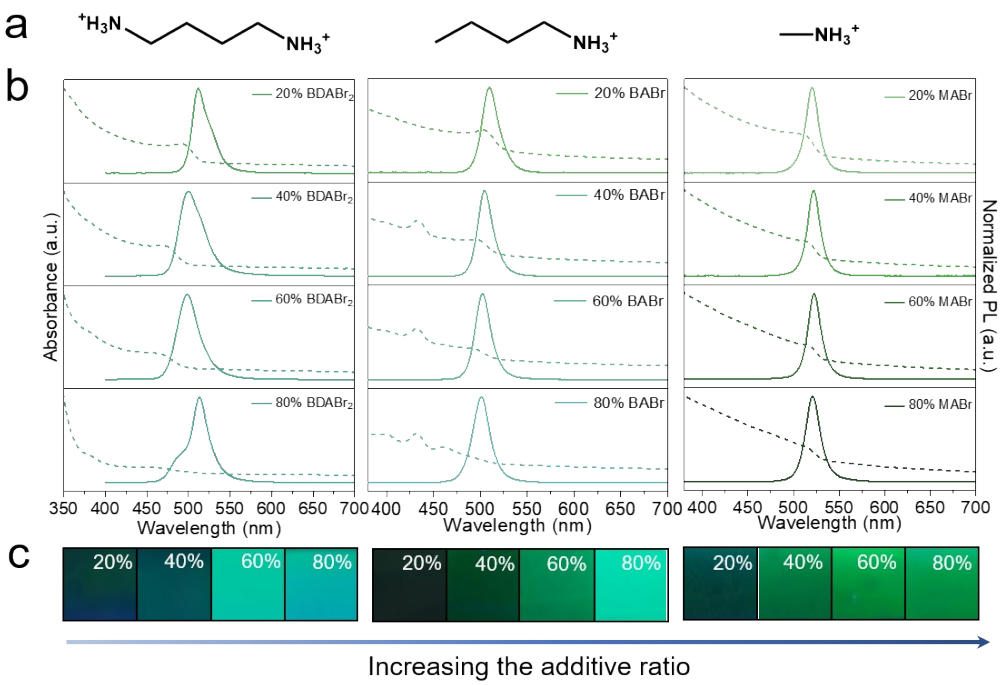

Figure S1. Optical characterizations of $CsPbBr_3$ films with different ammonium bromides and proportions. **a**, Molecular structure of BDA^{2+} , BA^{+} and MA^{+} cations. **b**, UV-vis absorption (dash line) and PL spectra (solid line) of the perovskite films. **c**, The corresponding digital images of the perovskite films under a 365 nm UV lamp. All the perovskite films were annealed before the test.

Since the incorporation of different ammonium cations may also result in the loading of different proportions of Br^- at the same time, one may concern that the Br^- will also affect the bandgap, crystal lattice, luminescence characteristics of the perovskite films. Although we could not completely exclude this possibility, we may rule out the main factor of different Br^- ratios determining the quality of perovskite emitters as below. Firstly, in these monoammonium bromides loaded perovskite films, such as PEABr, BABr, and EABr, when keeping the proportion of Br^- same, the perovskite films show quite different properties, as shown in Figure 1, Figure S1, Figure 2a, and Figure S2. In addition, the emission wavelength of the MABr-based films shows negligible difference with increasing the ratio of MABr, which may indicate that the Br^- has no impacts on the bandgap and crystal lattice of perovskites. Accordingly, it is safe for us to conclude that the ammonium cations should be the main factor determining the characteristics of the perovskite films rather than the proportion of Br^- anions.

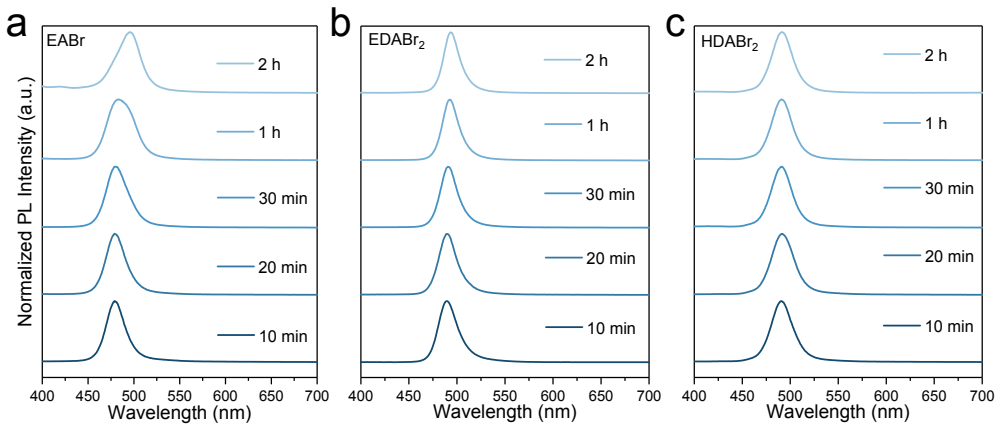

Figure S2. Normalized PL spectra of perovskite films with different ammonium bromides annealed at 80 ℃ for different time to estimate their thermal stability. **a**, EABr; **b**, $EDABr_2$; **c**, $HDABr_2$.

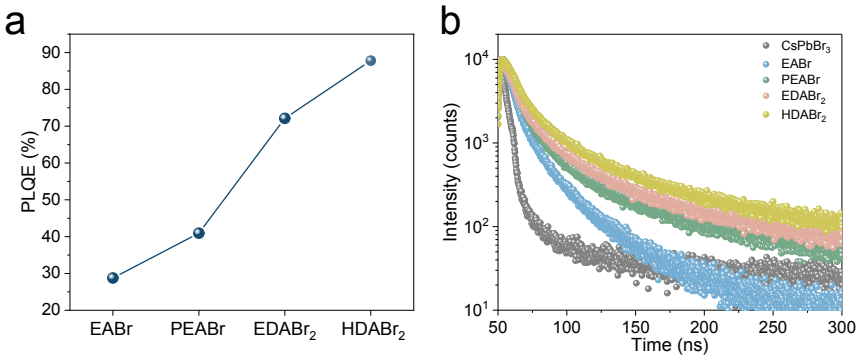

Figure S3. a, PLQEs of the sky-blue perovskite films with different ammonium bromides. The PLQEs were conducted with a 405 nm laser under a light intensity of ~0.2 mW cm^{-2}. **b**, TCSPC measurement of the sky-blue perovskite films. The fitted average lifetime were sumarrized in Table S3.

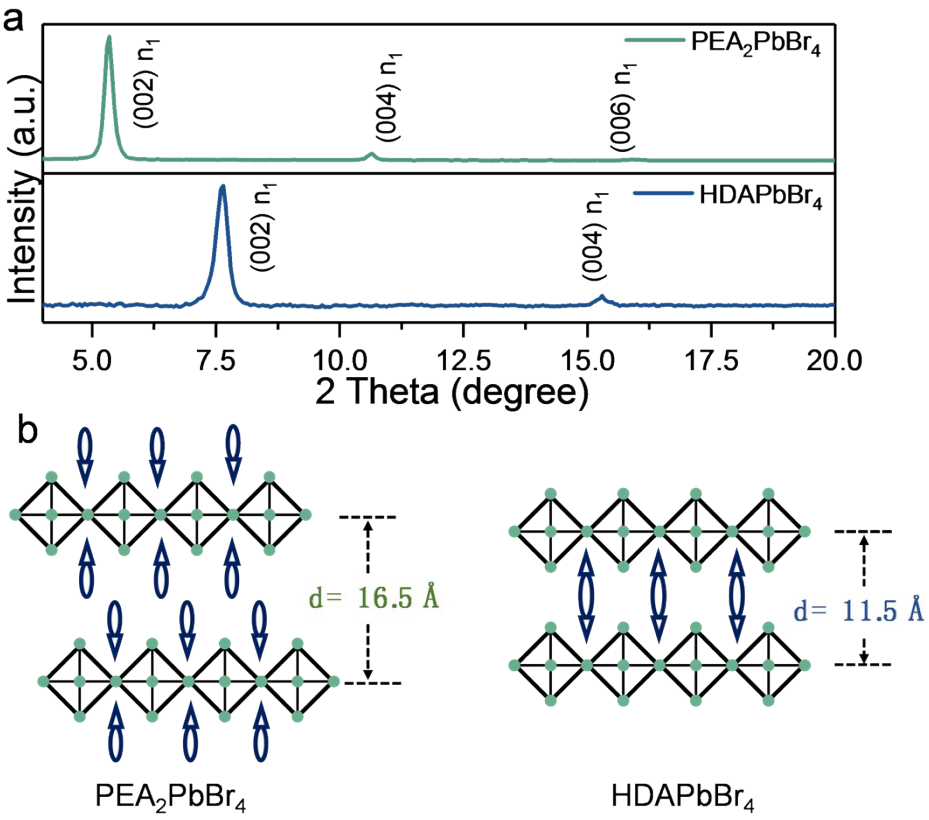

Figure S4. Characterizations of the PEA_2PbBr_4 (n = 1) and $HDAPbBr_4$ (n = 1) perovskite films. **a**, XRD patterns. **b**, Schematic illustration of structure and d-spacing of n = 1 low-dimensional R-P (left) and D-J (right) perovskites.

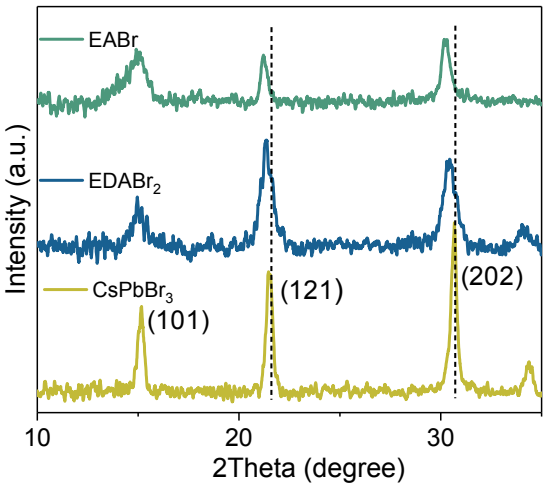

Figure S5. XRD patterns of control films and perovskite films with EABr and $EDABr_2$.

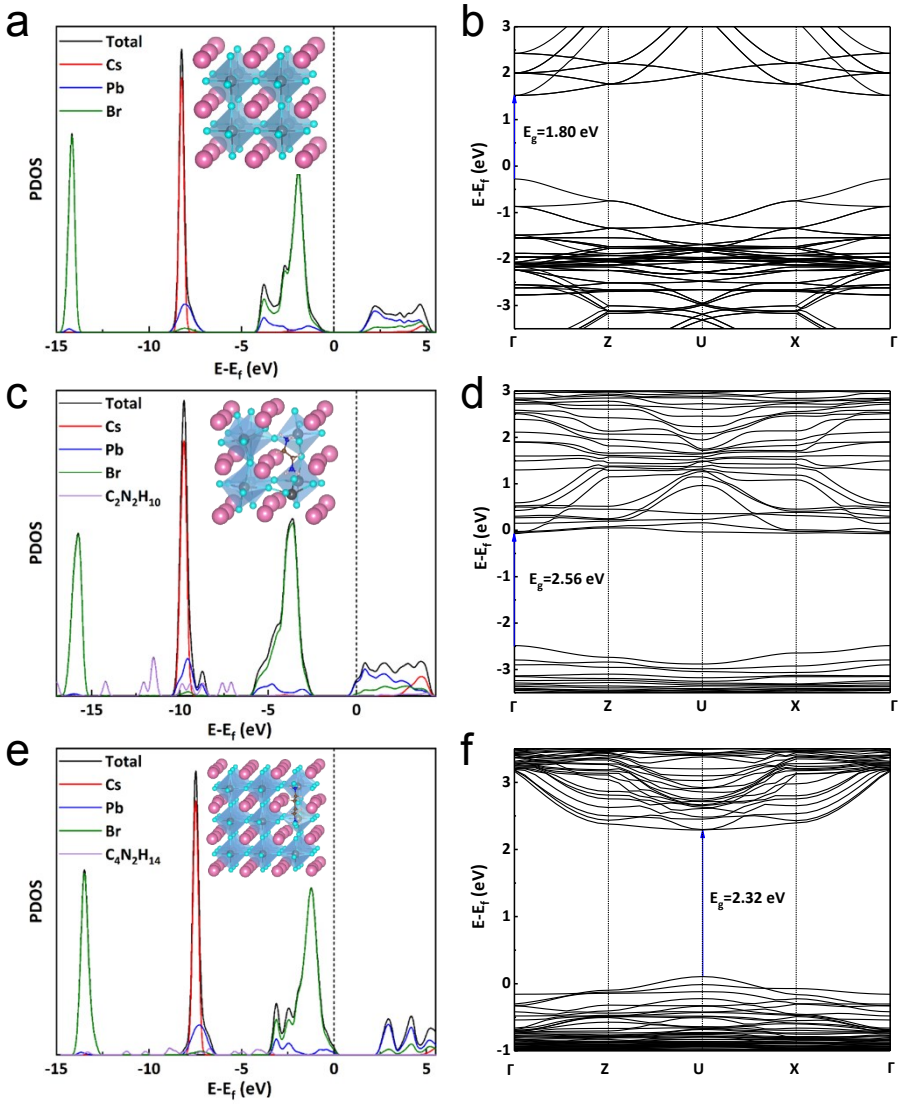

Figure S6. Simulated density of states (PDOS) and band structures from DFT calculations for **a-b**, $CsPbBr_3$ perovskite, **c-d**, EDA^{2+} incorporated and **e-f**, BDA^{2+} incorporated $CsPbBr_3$ perovskites. The Fermi level is defined at zero.

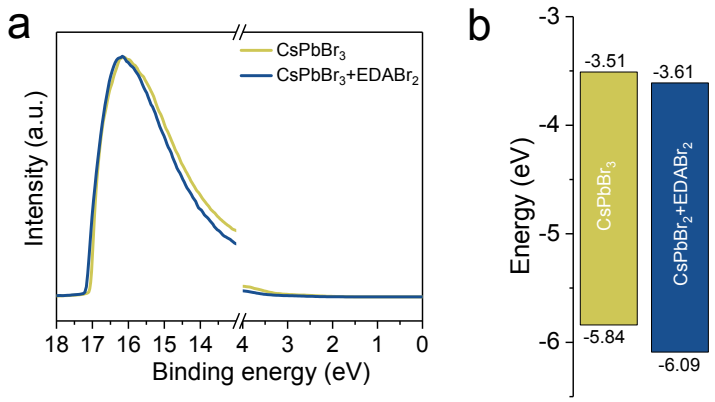

Figure S7. Characterization of the band structure of the control sample and EDA^{2+} incorporated "hollow" perovskite. **a**, UPS data. **b**, Schematic illustration of the VB and CB values of control and EDA^{2+} incorporated "hollow" perovskite.

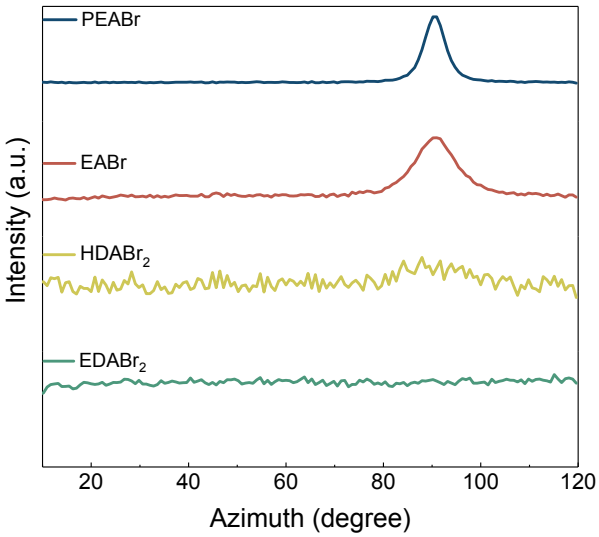

Figure S8. Azimuthal integration of (020) plane GIWAXS patterns in the $CsPbBr_3$ perovskite films with different ammonium bromides.

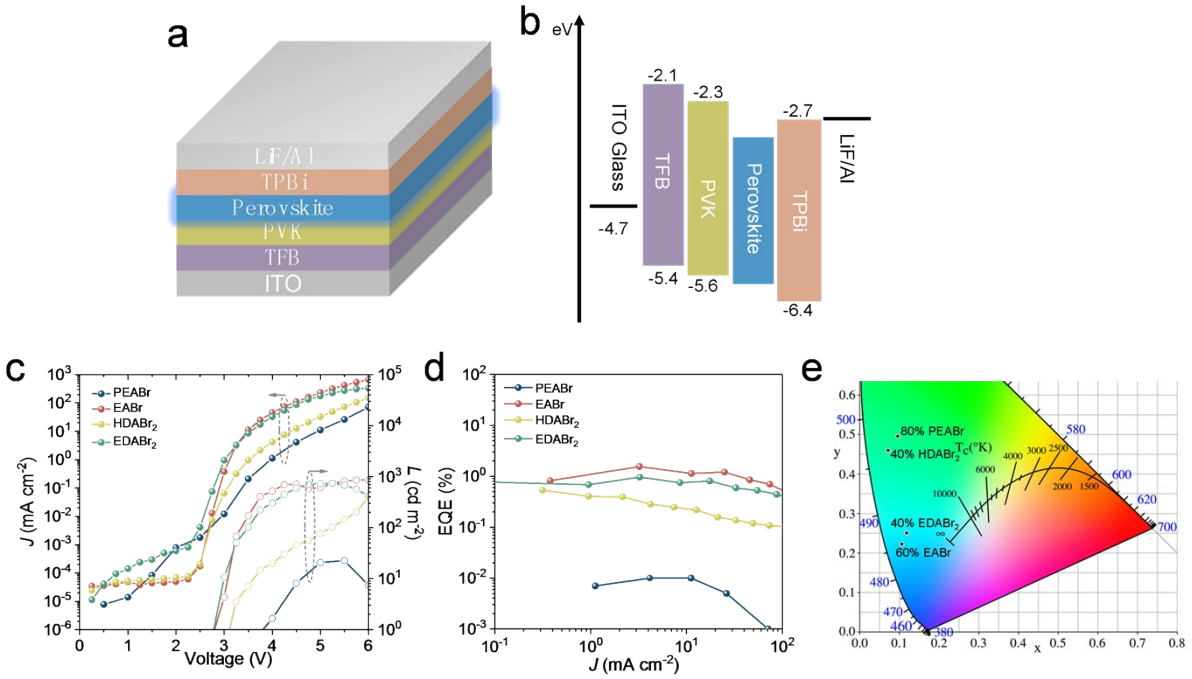

Figure S9. Characterizations of the performance of PeLEDs with different ammonium bromides. **a**, Device structure. **b**, Energy alignment. **c**, *J*-*V*-*L* curve. **d**, EQE-*J* curve. **e**, The corresponding CIE coordinates.

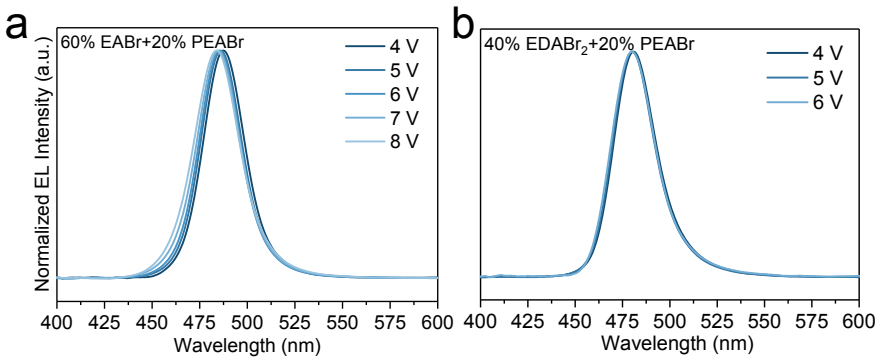

Figure S10. EL stability of EABr and $EDABr_2$ based PeELDs with additional PEABr. **a**, EABr. **b**, $EDABr_2$.

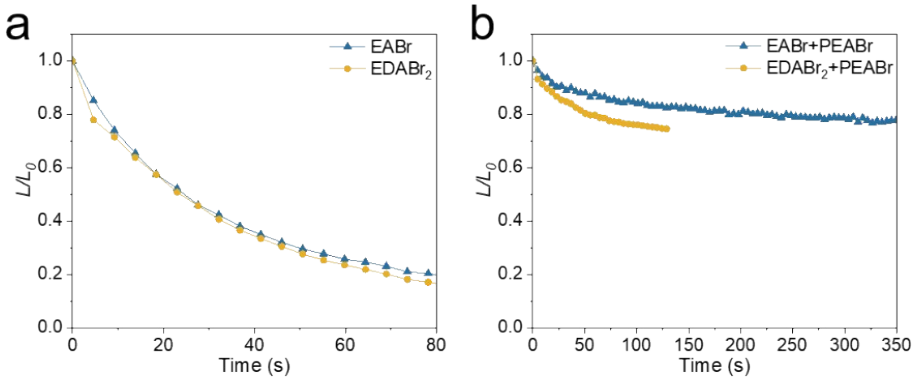

Figure S11. The luminance decay curves of blue perovskite devices with different additives. **a**, EABr or EDABr; **b**, Dual additives of PEABr and EABr or EDABr. An initial luminance of around 100 cd m^{-2} was set to measure the luminance decay.

Table S1. Summarized the effective ionic radii (r_{eff}) of perovskite and investigated ammonium cations, as well as the calculated tolerance factor (t) of different ammonium cations-formed perovskite.

Ions	Pb^{2+}	Br^-	Cs^+	EDA^{2+}	BDA^{2+}	HDA^{2+}	PEA^+	BA^+	EA^+	MA^+
r_{eff} (Å)	1.19	1.96	1.67	3.33	4.57	5.82	4.31	3.93	2.74	2.17
t			0.81	1.19	1.47	1.75	1.41	1.29	1.05	0.93

Table S2. Recipes for perovskite precursor solutions with different ratios of ammonium halides (MBr = PEABr, EABr, $HDABr_2$, $EDABr_2$, $BDABr_2$, BABr, and MABr).

Sample	CsBr [mmol mL^{-1}]	$PbBr_2$ [mmol mL^{-1}]	MBr [mmol mL^{-1}]
Control	0.2	0.2	-
20% MBr	0.2	0.2	0.04
40% MBr	0.2	0.2	0.08
60% MBr	0.2	0.2	0.12
80% MBr	0.2	0.2	0.16
100% MBr	0.2	0.2	0.20
120% MBr	0.2	0.2	0.24

Table S3. Summarized average PL lifetime ($\tau_{average}$), PLQE, and calculated radiative recombination rate k_r and nonradiative recombination rate k_{nr} of perovskite films fabricated with different ammonium cations. The PLQE measurements were conducted by using a PLQE test setup. The $\tau_{average}$ were extracted from PL decay curves in Figure S3, while the recombination rate k_r and k_{nr} were calculated from the equation of $\text{PLQE} = \frac{k_r}{k_r + k_{nr}}$ and $\tau_{average} = \frac{1}{k_r} + \frac{1}{k_{nr}}$.

Sample	k_r (ns $^{-1}$)	k_{nr} (ns $^{-1}$)	$\tau_{average}$ (ns)	PLQE (%)
EABr	0.09	0.22	15.4	29
PEABr	0.11	0.15	16.2	41
$EDABr_2$	0.15	0.06	24.2	72
$HDABr_2$	0.28	0.04	30.3	88